

Diffuse reflection of a Bose-Einstein condensate from a rough evanescent wave mirror

Hélène Perrin¹, Yves Colombe¹, Brigitte Mercier¹, Vincent Lorent¹ and Carsten Henkel²

¹ Laboratoire de Physique des Lasers, Université Paris 13
99 avenue Jean-Baptiste Clément, 93430 Villetaneuse, France

² Institut für Physik, Universität Potsdam
Am Neuen Palais 10, 14469 Potsdam, Germany

E-mail: henkel@uni-potsdam.de

Abstract. We present experimental results showing the diffuse reflection of a Bose-Einstein condensate from a rough mirror, consisting of a dielectric substrate supporting a blue-detuned evanescent wave. The scattering is anisotropic, more pronounced in the direction of the surface propagation of the evanescent wave. These results agree very well with theoretical predictions.

PACS numbers: 03.75.Nt, 32.80.Lg, 34.50.-s

Submitted to: *J. Phys. B: At. Mol. Opt. Phys.*

1. Introduction

The study of the interactions between ultra cold atoms and surfaces is of major interest in the context of Bose-Einstein condensation on microchips [1, 2]. One motivation is to understand the limitations on integrated matter wave devices due to imperfect surface fabrication or finite temperature. For example, it has been shown that the quality of the wires used in microfabricated chips is directly linked to the fragmentation effects observed in Bose-Einstein condensates (BECs) trapped near a metallic wire [3]. Moreover, the thermal fluctuations of the current in a metallic surface induce spin flip losses in an atomic cloud when the distance to the surface is smaller than 10 μm typically [4].

Dielectric surfaces and evanescent waves have also been explored for producing strong confinement. They have the advantage of a strong suppression of the spin flip loss mechanism compared to metallic structures [5]. With such a system, one can realize mirrors [6], diffraction gratings [7], 2D traps [8] or waveguides [9]. Experiments involving ultra cold atoms from a BEC at the vicinity of a dielectric surface have recently made significant progress, leading for instance to the realization of a two dimensional BEC [10], to the study of atom-surface reflection in the quantum regime [11], and to sensitive measurements of adsorbate-induced surface polarization [12] and of the Van der Waals/Casimir-Polder surface interaction [13].

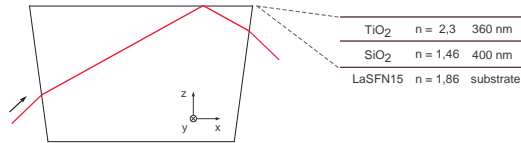


Figure 1. Dielectric prism supporting the evanescent wave. The surface is coated by two layers of successively low and high refractive index to realize a wave guide and enhance the evanescent field. For each incident polarization, TE or TM, coupling is resonant for a given incident angle. The experiments were performed with TE polarization. One denotes x as the propagation axis of the evanescent wave along the surface, y as the other horizontal axis and z as the vertical one.

In this paper, we present experimental results and a related theoretical analysis of Bose condensed Rubidium atoms interacting with the light field of an evanescent wave above a dielectric slab. The evanescent wave is detuned to the blue of an atomic transition line and provides a mirror for a BEC that is released from a trap and falls freely in the gravity field of the earth. After the bounce off the mirror, we observe a strong scattering of the atomic cloud (diffuse mirror reflection) that is due to the roughness of the slab surface where the evanescent wave is formed [14]. In our case, the phase front of the reflected matter waves is significantly distorted because the effective corrugation of the mirror is comparable to $\lambda_{dB}/4\pi \cos \theta$ where λ_{dB} is the incident de Broglie wavelength and θ the angle of incidence. This is similar to early experiments with evanescent waves [14] and with magnetic mirrors [15]. We mention that later experiments achieved a significantly reduced diffuse reflection (Arnold *et al* [16]) and were even able to distinguish a specularly reflected matter wave (Savalli *et al* [17]). The key result of our experiment is that we can quantitatively confirm the theoretical analysis developed by Henkel *et al* [18], combining independent measurements of the dielectric surface and the bouncing atoms.

The paper starts with a presentation of the experiment and an analysis of the experimental results, following Ref.[19]. We then outline an improved theoretical analysis based on Ref.[18] and discuss the momentum distribution of the reflected atoms, in particular its diffuse spread and its isotropy.

2. Setup

The evanescent wave is produced by total internal reflection of a Gaussian laser beam at the surface of a dielectric prism. As shown in Fig.1, the surface of the prism is coated by two dielectric layers, a TiO₂ layer on top of a SiO₂ spacer layer. This coating forms an optical waveguide that resonantly enhances the evanescent field above the top layer [20]; we have designed this configuration for the study of two-dimensional atom traps [21]. The incident angle of the laser beam is fixed by the resonance condition for a waveguide mode; for the transverse electric (or s) polarization we use, the incident angle is $\theta_i = 46.1^\circ$ (at the TiO₂/vacuum interface, index $n_{\text{TiO}_2} = 1.86$). The resulting exponential decay length of the light field is $\kappa^{-1} = 93.8$ nm, and $I = I_0 e^{-2\kappa z}$ is the light intensity.

The mirror light is produced by a laser diode of power 40 mW detuned 1.5 GHz above the atomic D2 line ($\lambda = 780$ nm or $1/\lambda = k_L/2\pi = 12\,820$ cm⁻¹). The Gaussian beam is elliptical and produces on the surface a spot with $1/\sqrt{e}$ waist diameters of

220 μm along x and 85 μm along y (see coordinate axes in Fig.1). A measurement of the reflection threshold for the atom beam, taking into account the van der Waals attraction toward the surface (Landragin *et al.* in Ref.[6]), gives access to the light intensity at the surface in the spot center: $I_0 = 210 \text{ W/cm}^2$. This value is lower than expected from the design of the dielectric coating; we attribute this to the losses due to the roughness of the deposited TiO_2 layer (see Figure 5 below and the discussion there).

3. Atom bounce

3.1. Data

The experiment proceeds as follows: approximately 10^8 atoms are confined in the hyperfine ground state $F = 2, m_F = 2$ in a Ioffe Pritchard (IP) type magnetic trap, 3.6 mm above the evanescent mirror [21]. The magnetic trap is cigar shaped, x being its long axis. Oscillation frequencies are, respectively, $\omega_x/2\pi = 21 \text{ Hz}$ and $\omega_\perp/2\pi = 220 \text{ Hz}$ in the radial directions (y and z). The atoms are evaporatively cooled to below the condensation threshold and about $N = 3 \times 10^5$ atoms are released at $t = 0$ by switching off the magnetic trapping fields. These atoms reach the mirror after free fall at $t_{\text{reb}} = 27 \text{ ms}$ and bounce on it with a velocity $v_i = 265 \text{ mm/s}$ (normal incidence $\theta = 0$, de Broglie wavelength $\lambda_{\text{dB}} = 2\pi\hbar/mv_i = 17.3 \text{ nm}$). Around the bouncing time t_{reb} , the mirror laser is switched on for $\Delta t = 2.2 \text{ ms}$. Limiting this time window Δt prevents near-resonant photon scattering during free fall or after reflection.

The atoms are detected by absorption imaging either before or after reflection. During free fall, the cloud expands along the radial directions because potential and interaction energy is released, but its width along x remains nearly constant. The analysis of pictures taken before reflection gives access to the following parameters: fraction of condensed atoms $N_0/N = 0.4$, kinetic temperature of thermal cloud $T = 285 \text{ nK}$, initial Thomas-Fermi size along x of the condensed fraction $R_x = 90 \mu\text{m}$ and Thomas-Fermi velocity width along z : $V_\perp = 5.96 \text{ mm/s}$. The condensate velocity width along x is very small, thus non directly measurable. However, it can be inferred from the knowledge of V_\perp and the oscillation frequencies in the magnetic trap, using the solution for an expanding BEC [22]; we get $V_x = \frac{\pi}{2} \frac{\omega_x}{\omega_\perp} V_\perp = 0.89 \text{ mm/s}$. The observation of the center of mass motion during free fall permits us to calibrate the pixel size knowing gravity's acceleration and to infer the initial position and velocity of the cloud. The magnetic field switching process communicates a small acceleration to the atoms along x , resulting in a horizontal velocity $v_x = -30.7 \text{ mm/s}$ (see Figure 2).

After reflection, the absorption images change dramatically (figure 2). The atoms occupy the surface of a scattering sphere, hence an elastic, but strongly diffuse scattering occurs. For $t > t_{\text{reb}}$, the cloud width along x increases from its initial value due to an additional velocity spread σ_{v_x} . The velocity Gaussian radius at $1/\sqrt{e}$ deduced from the pictures is 39.4 mm/s . Taking into account the initial velocity width before reflection, the spread due to diffuse reflection is $\sigma_{v_x} = 39 \text{ mm/s}$, that is $6.6 \pm 0.2 v_{\text{rec}}$ where $v_{\text{rec}} = \hbar k_L/m = 5.89 \text{ mm/s}$ is the recoil velocity for Rb. This corresponds to an angular (rms) spread $\Delta\theta \approx 8.4^\circ$.

The effect of diffuse reflection along y is more subtle to analyze, as this axis is aligned with the direction of observation. However, it is possible to extract information

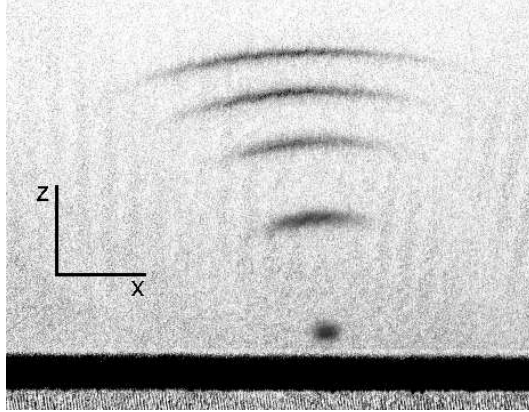


Figure 2. Absorption imaging pictures of a bouncing BEC with 3×10^5 atoms for different times of flight after reflection: 2 ms, 7 ms, 12 ms, 17 ms and 22 ms. The pictures, taken with a $200 \mu\text{s}$ long, resonant pulse, are merely superimposed. The wide black line in the bottom is due to the prism surface, slightly tilted from the imaging axis. Picture dimensions are $5.7 \text{ mm} \times 4.4 \text{ mm}$.

about σ_{v_y} from the picture. If for instance the scattering were totally isotropic, with $\sigma_{v_y} = \sigma_{v_x}$, the atomic cloud should extend asymmetrically towards $-z$ at a given position x , as the projection of a spherical shell onto a plane extends towards the inner part of the circle (see figure 4). If on the contrary the scattering would take place only along x , the cloud width along z at a given position x should be very small, with a symmetric shape.

3.2. Simulation

To get some insight into what happens along y , we performed a numerical simulation of the atomic reflection. The simulation calculates $N = 3 \times 10^5$ individual classical atomic trajectories. The initial positions and velocities are chosen to mimic the experimentally measured parameters: 40% of the atoms are “condensed” and are described by the initial 3D Thomas-Fermi velocity and position distribution. (We neglect the position spread along y and z because its contribution to the cloud size after a few ms of time of flight is very small.) The remaining 60% of the atoms are distributed according to gaussian profiles for velocity and position, with widths inferred from the knowledge of temperature and trap parameters. Position and velocity of the cloud centre are fixed to the experimental values as well. The mirror is modelled as an instantaneous diffuse reflector. This assumption is reasonable as the typical time spent in the evanescent wave is small, $1/\kappa v_i = 0.35 \mu\text{s}$. After reflection, the atomic velocity is modified to describe both specular reflection (inversion of vertical velocity) and scattering. A random horizontal velocity is added to the reflected velocity with a gaussian distribution. We take a $1/\sqrt{e}$ radius $\sigma_{v_x} = 39 \text{ mm/s}$, as measured experimentally, and run simulations with varying σ_{v_y} . The z component of the velocity is adjusted in order to preserve kinetic energy (the scattering process is elastic, total energy is conserved). The simulation also takes into account spontaneous emission. For our parameters, the atom spontaneously emits on average 0.13 photons per bounce [23]. We randomly draw the number of photons from a Poisson distribution and add a



Figure 3. Simulation of a bouncing BEC with 3×10^5 atoms for the same times of flight than the experimental ones, figure 2. For this series, the velocity spread was chosen to be $\sigma_{v_y} = \sigma_{v_x}/2 = 19.5$ mm/s. The position of the mirror surface is marked by a grey line.

recoil of $1 v_{\text{rec}}$ in a random direction in velocity space for each emission event. After calculation of all atomic trajectories, the atomic density profile is integrated along y as in the experimental pictures. We finally apply a Gaussian blur filter (width $\sigma_{\text{res}} = 9 \mu\text{m}$ along x and $20 \mu\text{m}$ along z) to mimic the finite resolution of the experimental imaging system that we calibrated independently.

3.3. Anisotropic scattering

The qualitative agreement between the experimental and simulated pictures is very good as can be seen on figure 3. To be more quantitative for the possible values of the velocity spread σ_{v_y} , we analyze the central part of the cloud. For each time of flight, a region of size $0.8 \text{ mm} \times 1.5 \text{ mm}$ along x and z respectively, centred on the maximum density of the cloud and identical for experimental and simulated pictures, is isolated and an integration of the signal is performed along x . We are left with a cut of the cloud along z , averaged over 0.8 mm along x . The experimental profile is compared to the simulated one, for different choices of σ_{v_y} after the bounce. Results are shown on figure 4 for a time of flight 59 ms.

The experimental data clearly exclude an isotropic diffuse reflection (figure 4, bold line). They also are different from the pure one dimensional scattering case (thin line): what fits best of all is a model intermediate between these two extremes, *i.e.* the scattering is only half as strong along y compared to x . The atom mirror thus has an angular reflection characteristic that is elongated in the direction parallel to the (real part of the) wave vector of the evanescent wave. Spontaneous emission plays only a minor role for our parameters, but we found that the agreement with the experimental density profiles is improved by taking it into account, in particular on the lower left wing of the peak.

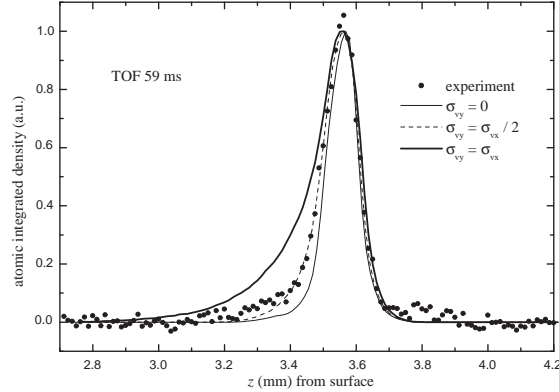


Figure 4. Atomic density profiles integrated along y and averaged along x , after 59 ms total time of flight, *i.e.* 32 ms after reflection. Closed circles: normalized experimental data. Lines: result of numerical calculation with a starting height 3.59 mm above the mirror, $N_0/N = 0.4$, $V_y = V_z = V_\perp = 5.96$ mm/s, $V_x = 0.89$ mm/s, $R_x = 90$ μ m, $T = 285$ nK, $v_x = -30.67$ mm/s, $v_z = 0.3$ mm/s and $\sigma_{v_x} = 39$ mm/s, values deduced from the experimental pictures. Thin line: totally anisotropic scattering ($\sigma_{v_y} = 0$); dashed line: anisotropic scattering with $\sigma_{v_y} = \sigma_{v_x}/2$; bold line: isotropic scattering ($\sigma_{v_y} = \sigma_{v_x}$). All curves are normalized to a maximum value of unity.

3.4. Mirror corrugation

For a theoretical prediction of the anisotropic mirror reflection, we use the theory of Ref.[18] where the diffuse scattering is attributed to the interference between the evanescent wave and light diffusely scattered from the rough glass surface. Within this theory, one can compute the width of the momentum distribution of the reflected atoms provided the power spectrum of the surface roughness is known. This power spectrum is a quantitative measure of the surface quality and has been measured with an atomic force microscope (AFM). A typical $4.5 \times 4.5 \mu\text{m}^2$ portion of the surface of the coated prism is shown in figure 5. One sees the top face of pillar-like structures which are typical for epitaxially grown TiO_2 on a substrate. The AFM data yield a surface roughness $\sigma = 3.34$ nm (the rms spread of the measured surface profile). A Fourier transform of the AFM image gives access to the power spectrum $P_S(\mathbf{Q})$. (We use capitalized boldface letters for two-dimensional vectors in the mirror plane.) It is found to be isotropic (a function of Q only) and well fitted in the wave vector range $1 k_L \dots 13 k_L$ by a power law with a low-frequency cut-off (see figure 6)

$$P_S(\mathbf{Q}) = \frac{P_0}{(1 + Q^2/Q_0^2)^{\alpha/2}} \quad (1)$$

The fit gives access to the parameters $\alpha = 4.8$, $P_0 = 5.3 \times 10^{-4} k_L^{-4}$ and $Q_0 = 4.94 k_L$. In terms of this power spectrum, the rms surface roughness σ is given by

$$\sigma^2 = \int \frac{d^2Q}{(2\pi)^2} P_S(\mathbf{Q}), \quad (2)$$

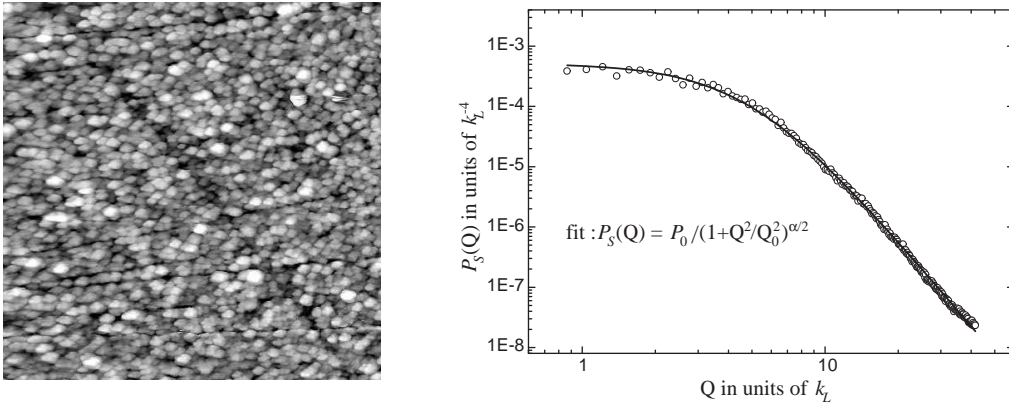


Figure 5. (left) Typical AFM picture of the prism surface. The dimensions are $4.5 \mu\text{m} \times 4.5 \mu\text{m}$. The grains are the top facets of pillar-like structures characteristic of an epitaxed TiO_2 surface.

Figure 6. (right) Open circles: Power spectrum $P_S(Q)$ deduced from the AFM measurement. Solid line: fit of the data by the function given at Eq.(1).

and the fitted parameters yield $\sigma = 3.36 \text{ nm}$, in excellent agreement with the value directly deduced from the rms spread of the AFM data.

3.5. Diffuse reflection theory and comparison to the data

We now show that the diffuse reflection we observe can be understood within the theory of Ref.[18]. We note first that the cloud is so dilute at the bounce that a single-atom picture is sufficient to capture the physics [24]. For a fixed incident momentum $\mathbf{p}_{\text{inc}} = \mathbf{P} - \mathbf{e}_z m v_i$ near normal incidence, the reflected wave function can be written in the form of a plane wave with a randomly modulated phase front:

$$\psi_{\text{refl}}(\mathbf{r}) = N \exp i [\mathbf{p}_{\text{spec}} \cdot \mathbf{r} + \delta\phi(\mathbf{R})], \quad (3)$$

where N is a normalization factor and $\mathbf{p}_{\text{spec}} = \mathbf{P} + \mathbf{e}_z m v_i$. (The dependence on the angle of incidence is actually negligible for our parameters [18].) The phase $\delta\phi(\mathbf{R})$ depends on the ‘impact position’ \mathbf{R} on the mirror, *i.e.*, the projection of \mathbf{r} onto the mirror plane. We perform an ensemble average over the realizations of the rough surface and compute the atomic momentum distribution $P_A(\mathbf{P} + \hbar\mathbf{Q})$ from the (spatial) Fourier transform of the ‘atomic coherence function’ (Sec. 6 of Ref.[18])

$$\begin{aligned} \langle \psi_{\text{refl}}^*(\mathbf{r}) \psi_{\text{refl}}(\mathbf{r}') \rangle &= N^2 \exp i [\mathbf{p}_{\text{spec}} \cdot (\mathbf{r}' - \mathbf{r})] \\ &\times \exp \left[-\frac{1}{2} \langle (\delta\phi(\mathbf{R}) - \delta\phi(\mathbf{R}'))^2 \rangle \right], \end{aligned} \quad (4)$$

(We take $\langle \delta\phi(\mathbf{R}) \rangle = 0$, assuming the roughness to be statistically homogeneous.) The variance of the phase shift can be found from the following formula (Eqs.(6.15) and

(5.16) of Ref.[18])

$$\langle \delta\phi(\mathbf{R})\delta\phi(\mathbf{R}') \rangle = \int \frac{d^2Q}{(2\pi)^2} P_S(\mathbf{Q}) |B_{\text{at}}(\mathbf{Q})|^2 e^{i\mathbf{Q}\cdot(\mathbf{R}-\mathbf{R}')}, \quad (5)$$

where $B_{\text{at}}(\mathbf{Q})$ is the ‘‘atomic response function’’ given in Eq.(5.15) of Ref.[18]. For the parameters of our experiment, we find that the phase shift has a variance $\langle \delta\phi^2(\mathbf{R}) \rangle = 16.5$ large compared to unity. In this regime, Ref.[18] has shown that the reflected atomic velocity distribution approaches a Gaussian shape whose width along the x -direction, for example, is given by

$$\frac{\sigma_{v_x}^2}{v_{\text{rec}}^2} = \frac{1}{k_L^2} \int \frac{d^2Q}{(2\pi)^2} Q_x^2 P_S(\mathbf{Q}) |B_{\text{at}}(\mathbf{Q})|^2. \quad (6)$$

This expression gives the additional broadening of the incident velocity distribution due to the diffuse mirror reflection. We perform the integration of Eq.(6) numerically, with the roughness power spectrum determined previously from the AFM images (Eq.(1)). For simplicity, we calculate the response function $B_{\text{at}}(\mathbf{Q})$ using scalar light scattering from the topmost interface only, ignoring the actual layered structure. We believe that this approximation is sufficient, at least for describing the scattering in the x -direction: as shown in Ref [18], the atom does not change its magnetic sublevel if it scatters in this direction and if the evanescent wave is linearly polarized. These conditions are met here so that both atom and light can be described by scalar wave fields.

Within the theoretical model outlined above, the velocity spread along the propagation direction of the evanescent wave is found to be $\sigma_{v_x} = 6.76 v_{\text{rec}}$. This value is in very good agreement with the experimental value $6.6 \pm 0.2 v_{\text{rec}}$. This is a very satisfying result because the theory only contains, within the approximations we made, parameters that are based on independent measurements. We believe that this is the first quantitative demonstration of evanescent wave scattering in the diffuse regime.

3.6. Discussion of the anisotropy

We also compute the anisotropy of the reflected atoms and find a ratio $\sigma_{v_x}/\sigma_{v_y} = 2.6$, in good agreement with the value (2 ± 0.5) extracted from the experimental data. As discussed in Ref.[18], this anisotropy arises from the fact that diffuse reflection occurs predominantly by Bragg transitions where a photon is absorbed from the evanescent wave (with wave vector $k_x = k_L n_{\text{TiO}_2} \sin\theta_i$) and another photon is emitted into a diffusely scattered mode that emerges at grazing incidence into the vacuum half-space (or the inverse process). If these scattered modes are distributed isotropically in the mirror plane on a circle of radius $r_{\text{sc}}k_L$, the ratio of the rms spreads would be $\sigma_{v_x}/\sigma_{v_y} = (2(n_{\text{TiO}_2} \sin(\theta_i)/r_{\text{sc}})^2 + 1)^{1/2}$. Taking $r_{\text{sc}} = 1$, which corresponds to scattered modes emerging at grazing incidence, we again find an anisotropy ratio of ≈ 2.5 . This agreement is not very surprising since the rough surface has a power spectrum much broader than the photon wavenumber k_L (Fig.6). Within this simple calculation, however, we can also get a quick estimate of the impact of the dielectric coating. The choice $r_{\text{sc}} = n_{\text{TiO}_2} \sin(\theta_i)$ corresponds to resonant scattering into waveguide modes in the TiO_2 layer and leads to a ratio $\sigma_{v_x}/\sigma_{v_y} = \sqrt{3}$ which cannot be excluded experimentally.

4. Conclusion

In conclusion, we have observed the diffuse reflection of an ultracold atomic beam from an evanescent wave. The wave propagates on the rough surface of a dielectric prism, and light scattering leads to an atom mirror showing a significantly nonspecular reflection. The angular broadening of the reflected atoms, as well as their anisotropic angular distribution in the mirror plane, are in good agreement with a theory developed by Henkel *et al.* [18]. It is remarkable that this agreement does not imply any free parameters since we independently measured the spectrum of the surface roughness with an AFM. In our experiment, using a BEC has mainly practical advantages. Indeed, as we mentioned above, everything can be understood within a single-atom picture, and after diffuse scattering, spatial coherence is seriously reduced, as is discussed in Ref.[18] and investigated in Ref.[25]. Nevertheless, the BEC provides crucial advantages because we achieve a very clean situation. Apart from a very low velocity spread $V_x \ll \sigma_{v_x}$, a BEC has a negligible size when impacting the evanescent wave surface. This removes the need to take into account the mirror curvature due to the gaussian spot profile; the contribution of the initial size to the cloud width after reflection is negligible; and the losses given the finite size of the mirror (the waist of the reflected laser beam) are minimal. In fact, with a freely falling, ultracold, but thermal gas, the finite mirror size would lead to strongly reduced signal.

Acknowledgments

We gratefully acknowledge support by the Région Ile-de-France (contract number E1213) and by the European Community through the Research Training Network “FASTNet” under contract No. HPRN-CT-2002-00304 and the Marie Curie Research Network “Atom Chips” under contract No. MRTN-CT-2003-505032. Laboratoire de Physique des Lasers (LPL) is Unité Mixte de Recherche 7538 of Centre National de la Recherche Scientifique and Université Paris 13. The LPL group is a member of the Institut Francilien de Recherche des Atomes Froids.

- [1] Hänsel W, Hommelhoff P, Hänsch T W and Reichel J 2001 *Nature* **413** 498–501
- [2] Folman R, Krüger P, Schmiedmayer J, Denschlag J H and Henkel C 2002 *Adv. At. Mol. Opt. Phys.* **48** 263–356
- [3] Fortágh J, Ott H, Kraft S and Zimmermann C 2002 *Phys. Rev. A* **66** 041604(R)
Leanhardt A E, Shin Y, Chikkatur A P, Kielpinski D, Ketterle W and Pritchard D E 2003 *Phys. Rev. Lett.* **90** 100404
Schumm T, Estève J, Figl C, Trebbia J B, Aussibal C, Nguyen H, Maily D, Bouchoule I, Westbrook C and Aspect A 2005 *Eur. Phys. J. D* **32** 171–80
- [4] Jones M P A, Vale C J, Sahagun D, Hall B V and Hinds E A 2003 *Phys. Rev. Lett.* **91** 080401
Harber D M, McGuirk J M, Obrecht J M and Cornell E A 2003 *J. Low Temp. Phys.* **133** 229–38
Rekdal P K, Scheel S, Knight P L and Hinds E A 2004 *Phys. Rev. A* **70** 013811
- [5] Henkel C and Wilkens M 1999 *Europhys. Lett.* **47** 414–20
Henkel C, Pötting S and Wilkens M 1999 *Appl. Phys. B* **69** 379–87
- [6] Balykin V I, Letokhov V S, Ovchinnikov Y B and Sidorov A I 1988 *Phys. Rev. Lett.* **60** 2137–40
Kasevich M A, Weiss D S and Chu S 1990 *Opt. Lett.* **15** 607–609
Aminoff C G, Steane A M, Bouyer P, Desbiolles P, Dalibard J and Cohen-Tannoudji C 1993 *Phys. Rev. Lett.* **71** 3083–6
Landragin A, Courtois J Y, Labeyrie G, Vansteenkiste N, Westbrook C I and Aspect A 1996 *Phys. Rev. Lett.* **77** 1464–7
- [7] Christ M, Scholz A, Schiffer M, Deutschmann R and Ertmer W 1994 *Opt. Commun.* **107** 211–7
Brouri R, Asimov R, Gorlicki M, Feron S, Reinhardt J, Lorent V and Haberland H 1996 *Opt. Commun.* **124** 448–51

- Szriftgiser P, Guéry-Odelin D, Arndt M and Dalibard J 1996 *Phys. Rev. Lett.* **77** 4–7
- Cognet L, Savalli V, Horvath G Z K, Holleville D, Marani R, Westbrook N, Westbrook C I and Aspect A 1998 *Phys. Rev. Lett.* **81** 5044–5047
- [8] Ovchinnikov Y B, Shul'ga S V and Balykin V I 1991 *J. Phys. B: Atom. Mol. Opt. Phys.* **24** 3173–8
- Gauck H, Hartl M, Schneble D, Schnitzler H, Pfau T and Mlynek J 1998 *Phys. Rev. Lett.* **81** 5298–301
- Hammes M, Rychtarik D, Engeser B, Nägerl H C and Grimm R 2003 *Phys. Rev. Lett.* **90** 173001
- [9] Dekker N H, Lee C S, Lorent V, Thywissen J H, Smith S P, Drndić M, Westervelt R M and Prentiss M 2000 *Phys. Rev. Lett.* **84** 1124–7
- [10] Rychtarik D, Engeser B, Nägerl H C and Grimm R 2004 *Phys. Rev. Lett.* **92** 173003
- [11] Pasquini T A, Shin Y I, Sanner C, Saba M, Schirotzek A, Pritchard D E and Ketterle W 2004 *Phys. Rev. Lett.* **93** 223201
- Pasquini T A, Saba M, Jo G, Shin Y, Ketterle K, Pritchard D E, Savas T A and Mulders N 2006, “Low velocity quantum reflection of Bose-Einstein condensates” *preprint* cond-mat/0603463.
- [12] McGuirk J M, Harber D M, Obrecht J M and Cornell E A 2004 *Phys. Rev. A* **69** 062905
- [13] Lin Y J, Teper I, Chin C and Vuletić V 2004 *Phys. Rev. Lett.* **92** 050404
- Harber D M, Obrecht J M, McGuirk J M and Cornell E A 2005 *Phys. Rev. A* **72** 033610
- Obrecht J M, Wild R J, Antezza M, Pitaevskii L P, Stringari S and Cornell E A 2006, “Measurement of the Temperature Dependence of the Casimir-Polder Force” *preprint* physics/0608074.
- [14] Landragin A, Labeyrie G, Henkel C, Kaiser R, Vansteenkiste N, Westbrook C I and Aspect A 1996 *Opt. Lett.* **21** 1581–3
- In these experiments, some indications for anisotropic scattering after reflection of thermal atoms on an evanescent wave mirror were observed (C. Westbrook and A. Landragin, private communication).
- [15] Hinds E A and Hughes I G 1999, *J. Phys. D: Appl. Phys.* **32** R119–46
- [16] Arnold A S, MacCormick C and Boshier M G 2002, *Phys. Rev. A* **65** 031601
- [17] Savalli V, Stevens D, Estève J, Featonby P D, Josse V, Westbrook N, Westbrook C I and Aspect A 2002 *Phys. Rev. Lett.* **88** 250404
- [18] Henkel C, Mølmer K, Kaiser R, Vansteenkiste N, Westbrook C I and Aspect A 1997 *Phys. Rev. A* **55** 1160–78
- [19] Perrin H, Colombe Y, Mercier B, Lorent V and Henkel C 2005 *J. Phys.: Conf. Ser.* **19** 151–7; doi:10.1088/1742-6596/19/1/025, *preprint* quant-ph/0509200
- [20] Kaiser R, Lévy Y, Vansteenkiste N, Aspect A, Seifert W, Leipold D and Mlynek J 1994 *Opt. Commun.* **104** 234
- [21] Colombe Y, Kadio D, Olshanii M, Mercier B, Lorent V and Perrin H 2003 *J. Opt. B: Quantum Semiclass. Opt.* **5** S155–63
- [22] Castin Y and Dum R 1996 *Phys. Rev. Lett.* **77** 5315–9
- Kagan Y, Surkov E L and Shlyapnikov G V 1996 *Phys. Rev. A* **54** R1753–6
- [23] This value is deduced from an integration of the number of scattered photons along the mean classical atomic trajectory, calculated from the known evanescent wave parameters. We neglect the variation of the spontaneous emission rate at the vicinity of the surface. This assumption is reasonable as the classical turning point is rather far from the surface ($k_L z_0 = 1.33$). See Henkel C and Courtois J-Y 1998 *Eur. Phys. J. D* **3** 129–153.
- [24] Bongs K, Burger S, Birkel G, Sengstock K, Ertmer W, Rzazewski K, Sanpera A, and Lewenstein M 1999 *Phys. Rev. Lett.* **83** 3577; Busch T, private communication
- [25] Estève J, Stevens D, Aussibal C, Westbrook N, Aspect A and Westbrook C I 2004 *Eur. Phys. J. D* **31** 487–91